



## Thermodynamic evaluation of fixed charge density and dielectric properties of PVC based $Mn_3(PO_4)_2$ composite ion-exchange membrane

Mohd Arsalan, Mohd Zeeshan, Rafiuddin\*

Membrane Research Laboratory, Department of Chemistry, Aligarh Muslim University, Aligarh 202002, India, Tel./Fax: +91 571 2703515; email: [mohdarsalan.chem@gmail.com](mailto:mohdarsalan.chem@gmail.com) (M. Arsalan), Tel./Fax: +91 09760229165; email: [mohd.zee2010@gmail.com](mailto:mohd.zee2010@gmail.com) (M. Zeeshan), Tel./Fax: +91 9760640655; email: [rafi\\_amu@yahoo.com](mailto:rafi_amu@yahoo.com) (Rafiuddin)

Received 24 March 2014; Accepted 5 November 2014

### ABSTRACT

PVC based MP composite membrane has been prepared by the sol–gel method of material synthesis. This composite material as well as membrane has been characterized by SEM, XRD, FTIR, TGA, and LCR studies which are used to show the mechanical, chemical, and thermal properties. By the above characterizations, it is clear that the membrane has smooth, porous, and cracks free surface as well as it also verified the material nature, functional groups, thermal stability, phase transition, ion transportation etc. Some strong electrolytes are used to obtain the ionic potential and charge density of membrane which decided the nature of charge present on membrane. TMS theoretical approach is used to obtain the other parameters of membrane like transport number, mobility ratio, charge effectiveness etc. The observed ionic potential and charge density of used electrolytes are following the  $KCl < NaCl < LiCl$  and  $KCl > NaCl > LiCl$  order, respectively.

*Keywords:* Sol–gel method; PVC based MP composite material; TGA analysis; Mechanical and electrical properties; Charge density

### 1. Introduction

Ion-exchange composite membranes have much application in various fields like chemicals, foods, drugs, electro-dialysis, membrane electrolysis, desalination, diffusion, electro-deionization, electrochemical synthesis, fuel cells, storage batteries etc. Such types of composite membranes are also more functional in the field of textiles, beverages, pharmacies, medicines, and wastewater treatment [1–5]. Due to high thermal, chemical, and mechanical stabilities, it has much importance to show very applicable properties in the field of water purification and filtration technology.

The organic–inorganic composite membranes have been designed by a uniform mixing of organic polymers and inorganic particles into a particular ratio of percentages. Therefore, such type of membranes exhibit the important properties of both the used organic–inorganic constituents [6]. In this study, PVC provides the backbone structure and flexibility, while MP gives the particular ion-exchange property as well as thermal stability. By these above characteristics, the prepared composite membrane has very unique electrochemical, chemical, optical, magnetic, thermal, and mechanical stabilities as well as excellent selectivity for heavy toxic metal and electrolyte ions [7–10].

A wide range of membrane separation techniques like filtrations that are microfiltration, nanofiltration,

\*Corresponding author.

ultrafiltration, gas separation, and reverse osmosis have already been studied and industrially used [11–13]. The most important property of such type of ion-exchange membrane is to selectively permeate the cations or anions with respect to their charges. To examine the conductivity, selectivity, and mechanical property, the membrane must absorb the significant amount of water to assist the easy ionic migration. The high water uptake of membrane makes it mechanically unstable and less selective, which means that the morphology of membrane shows great influence on their applicability and performances [14]. The electrochemical performance and cost parameter are the important characteristics of a well-stable ion-exchange composite membrane. The chemical stability of membrane has been examined by exposing it into the different harsh or modest pH solutions [15].

The observation of membrane potential is an important criterion which characterizes the ions transport property through the charged membrane [16]. If membrane comes into the contact of aqueous or unequal electrolyte solutions, it acquires an electric charge through several possible mechanisms like dissociation of functional groups, adsorption of polyelectrolyte and ions, charged macro molecules, ionic surfactants etc. The potential observation is a simple and prominent method which describes the transport phenomena through charged membrane that is theoretically predicted by TMS method [17].

## 2. Theory

### 2.1. Teorell–Meyer–Sievers theoretical method

In TMS theory, there is an equilibrium development taking place at the solution and membrane interfaces which has a proper similarity with the donnan equilibrium. The assumptions which are made are described as follows:

- (a) The mobility of ions and concentration of fixed charges are constant throughout the membrane phase and it is independent of the salt concentration.

- (b) The water transference from the used solutions may be neglected.

The implications of these assumptions have been discussed earlier [18]. But further assumptions that are the activity coefficient of salt is similar in solution as well as membrane phase along with interface made there. The introduction of activities for concentration can be corrected by donnan potential either using the integration of Planck’s or Henderson equations. According to TMS theory, membrane potential is given by the following equation:

$$\Delta\bar{\psi}_m = 59.2 \left( \log \frac{C_2}{C_1} \frac{\sqrt{4C_1^2 + \bar{D}^2 + \bar{D}}}{\sqrt{4C_2^2 + \bar{D}^2 + \bar{D}}} + \bar{U} \log \frac{\sqrt{4C_2^2 + \bar{D}^2 + \bar{D}\bar{U}}}{\sqrt{4C_1^2 + \bar{D}^2 + \bar{D}\bar{U}}} \right) \tag{1}$$

where

$$\bar{U} = (\bar{u} - \bar{v}) / (\bar{u} + \bar{v}) \tag{2}$$

where  $\bar{u}$  and  $\bar{v}$  are the ionic mobility’s of cations and anions ( $m^2/v/s$ ), respectively, in the membrane phase.  $C_1$  and  $C_2$  are the concentrations of electrolyte solutions on either side of membrane and  $\bar{D}$  is the charge density of membrane which is expressed in eq/L. The graphical method of TMS determines the fixed charge density and cations to anions mobility ratio in membrane phase. The used electrochemical setup is represented by Fig. 1 which indicated that the charged membrane has been placed at the center of a measuring cell that has two glass chambers of 35 mL capacity [19,20].

## 3. Experimental

### 3.1. Preparation of composite membrane

MP precipitated material has been synthesized by the mixing of 0.2 M  $MnCl_2$  (Otto Kemi-India with

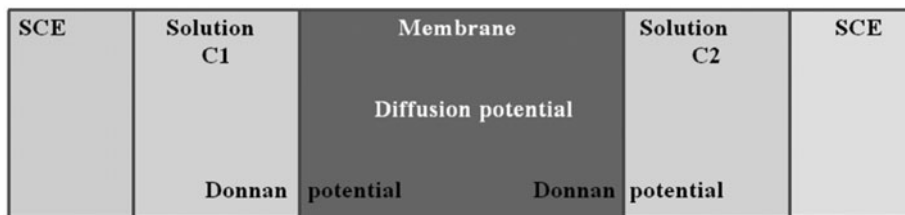


Fig. 1. Electrochemical setup for ionic potential measurement.

purity of 99.989%) with 0.2 M  $\text{Na}_3\text{PO}_4$  (E. Merck-India with purity of 99.90%) solution. By the mixing of these above  $\text{MnCl}_2$  and  $\text{Na}_3\text{PO}_4$  solutions, it gets converted into the MP precipitated solution. The precipitated material has been filtered through Whatman filter paper and then it must be well washed nearly 3–4 times by deionised water to eliminate the free electrolytes and ions. Latterly, it has been placed into an oven for 2–3 h by maintaining  $100^\circ\text{C}$  temperature. After that, the material has been crushed into fine powder with the help of pestle and mortar. By potential observation, it was clear that the resulting powdered material shows good ion-exchange property plus mechanical stability and it has increased flexibility plus binding ability after adding the PVC binder. The size of both the PVC and MP powdered material must have 200 meshes and it should be completely mixed with each other which results to make a stable composite membrane. There should be an appropriate ratio of binder and inorganic material which must be dried under a proper condition of temperature. Lastly, the composite material has been transferred into a cast die to apply pressure for the formation of ideal size composite membrane. The membrane has then incubated into a glass cell to observe the ionic potential of used electrolyte solutions through digital potentiometer. Our main effort has been to get the membrane of adequate chemical and mechanical stability. So, the membrane which has been prepared by embedding the 25 and 75% of PVC and MP materials, respectively, indicated good mechanical stability and functions. If it contains (>25% or <25%) of PVC binder, it cannot give appropriate stability and functions. Furthermore, this composite membrane has been subjected to microscopic and electrochemical characterization to see the morphology and mechanical stability [21,22].

### 3.2. Potential observation

Membrane potential has been observed by using the digital “Electronics India-118” potentiometer. The freshly prepared charged membrane has been installed at the center of a glass cell which has two chambers on either side. The various salt solutions such as chlorides of  $\text{K}^+$ ,  $\text{Na}^+$ , and  $\text{Li}^+$  are used to show the ionic potential. The collar-shaped glass chambers have the cavity to introduce the electrolyte solutions and saturated calomel electrodes. Each chamber of glass cell contains 25 mL of solution, while the capacity of it is near about 35 mL.

### 3.3. Measurement of membrane conductance

The electrical conductance of such type of membrane has been measured by the method which has already been used by various authors [23]. The membrane was sealed between the two Pyrex glasses half cells which were first filled with electrolyte solutions of known concentration to equilibrate the membrane and then has been replaced by the purified mercury without removing the adhering surface liquid. Platinum electrodes which kept dipped into the mercury are used to establish electrical contact. The membrane conductance has monitored on a direct reading of conductivity meter “Model No. L303”. The solutions in both compartments have been vigorously stirred by the magnetic stirrers at a constant 500 rpm to minimize the effect of boundary layers. The whole cells assembly has been kept immersed in a water thermo state through maintaining the required temperature of  $10\text{--}50^\circ\text{C}$ .

## 4. Characterization of membrane

### 4.1. Physico-chemical characterization of membrane

#### 4.1.1. Measurement of thickness and swelling

The thickness of membrane has been obtained by measuring the average thickness of 4–5th replicates by using screw gauze apparatus. The swelling was also measured by taking the differences between the average thickness of membrane which was equilibrated with 1 M NaCl solution for 24 h and the dry membrane.

#### 4.1.2. Measurement of water absorption and water flux

Firstly, the membrane has been kept in water for soaking the water to diffusible salt, and further, it has been blotted quickly with Whatmann filter paper to remove the moisture of the surface and immediately weighted. The membrane was further dried at a constant weight in a vacuum over  $\text{P}_2\text{O}_5$  for 24 h. So the water absorption of membrane has been calculated by the following equation:

$$\text{Water absorption (\%)} = \left[ \frac{W_{\text{wet}} - W_{\text{dry}}}{W_{\text{dry}}} \right] \times 100 \quad (3)$$

where  $W_{\text{wet}}$  is the weight of swollen membrane which was obtained by soaking water for 5 h, and  $W_{\text{dry}}$  is the weight of dry membrane. The water flux has been measured easily under a pressure difference of

0.2 MPa at an ambient temperature and easily calculated by using the equation:

$$F = V/At \quad (4)$$

where  $V$  is the total volume of water permeated during the experiment,  $t$  is operation time, and  $A$  is the membrane surface area.

#### 4.1.3. Porosity

Porosity is the volume of incorporated water in cavities of membrane as per unit volume from the water content data:

$$\text{Porosity (\%)} = \left[ \frac{W_{\text{wet}} - W_{\text{dry}}}{AL\rho_w} \right] \times 100 \quad (5)$$

$A$  = area of membrane,  $L$  = thickness the membrane, and  $\rho_w$  = density of water.

#### 4.2. Chemical stability

Chemical stability was evaluated on the basis of "ASTMD543-95" method. In this method, the membrane has been exposed into the several media like acidic, basic, and alkaline solutions. It has been evaluated after passing the 24, 36, and 48 h which analyzes the alteration in color, texture, brightness, decomposition, splits, holes, bubbles, curving, and stickiness etc. [24,25].

#### 4.3. SEM investigation of membrane morphology

Scanning electron microscopy images were used to confirm the microstructure of fabricated porous membrane. The membrane morphology was investigated by "Leo 4352" at an accelerating voltage of 20 kV. The sample was mounted on a copper stub and sputter coated with gold to minimize the charging.

#### 4.4. X-ray diffraction study of composite material

X-ray diffraction pattern of PVC based MP composite material was recorded by the "Miniflex-II X-ray diffractometer" Rigaku Corporation, with Cu K $\alpha$  radiation.

#### 4.5. FTIR analysis of composite material

The FTIR spectrum of pure PVC and PVC based MP composite material was done by "Interspec 2020

FTIR-spectrometer' spectrolab-UK. In this model, the sample compartment is 200 mm wide, 290 mm deep, and 255 mm high. The entrance and exit beam of sample compartment is sealed with a coated KBr window and a hinged cover present which are used to protect it from external environment.

#### 4.6. Thermo gravimetric analysis of composite material

The degradation process as well as thermal stability of PVC based MP composite membrane was investigated by using "Shimadzu DTG-60H" under the nitrogen atmosphere by using a heating rate of 20°C min<sup>-1</sup> from the temperature 25–800°C.

#### 4.7. Dielectric properties of composite membrane

The dielectric properties as well as impedance measurement was made from 75 kHz up to 5 MHz by using the Agilent "Model; 4284A" precision LCR meter.

### 5. Results and discussion

SEM images of PVC based MP composite membrane which has been prepared at 100 MPa applied pressure are shown in Fig. 2(a) and (b). Through the images, it is clear that the PVC based MP composite membrane has resistance to compaction and there is no visible breakage or cracks and swellings found on the surface. The information obtained by SEM images has provided the direction of well-ordered material preparation, micro or macro porosity, thickness, homogeneity, surface texture etc. [26,27]. The composite powder sample has been mounted in a sample holder by glass slides and the pattern has been recorded by using a "Rigaku Miniflex X-ray diffractometer" with Cu K $\alpha$  radiation ( $\lambda = 1.54060 \text{ \AA}$ ) in  $2\theta$  range from 20° to 80°. It has indicated the structure and lattice parameter of composite sample. The XRD spectrum of PVC based MP composite is depicted in Fig. 3, through which the present spectra indicated that the most intense peak found at  $2\theta = 26.30^\circ$  corresponds to (2 1 1) plane of composite sample [28]. Crystallite size of sample was found at near about ~26.8 nm range which has been calculated from the most intense peak value. The presence of intense peak in spectra indicated that the particles of material were present in crystalline form.

FTIR spectra are used as an important tool to provide the detail of binding sites as well as various significant bands of functional groups which are present in the composite material. The spectra of only PVC



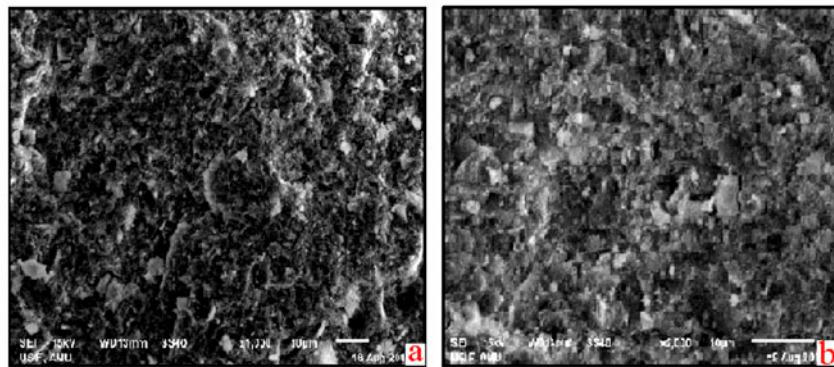


Fig. 2. SEM images (a and b) of PVC based MP composite membrane at different magnifications.

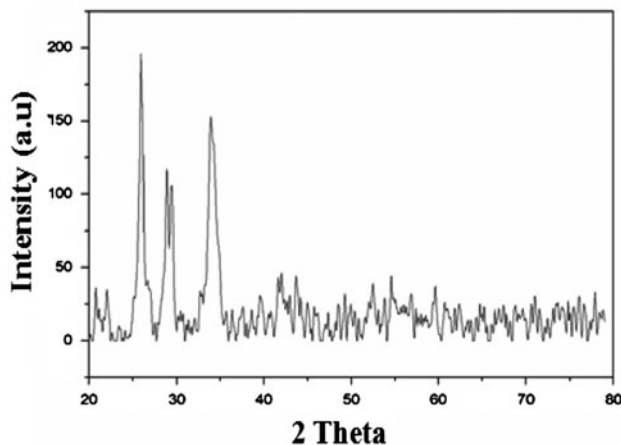


Fig. 3. XRD spectra of the PVC based MP composite material.

and PVC based MP material are, respectively, present in Fig. 4(a) and (b). In the first one, there is a peak present at the range from 1,066.12 to 1,387.42  $\text{cm}^{-1}$  which shows the C–H bond of polymer, where as another peak is found at the range of 816.64–471.63  $\text{cm}^{-1}$  indicated the presence of C–Cl bond, and the bands at 1,565.82–1,649.08 shows the presence of methyl ( $-\text{CH}_3$ ) group. Sample (4b), which is PVC based MP material, shows a broad peak at the range of 1,010.80–1,066.30  $\text{cm}^{-1}$  indicating the presence of C–H bonds in composite material. The peak at 582.64  $\text{cm}^{-1}$  shows the presence of phosphate group and a less intense peak is found at the 1,613.40  $\text{cm}^{-1}$  indicating the presence of methyl group. The broad peak which was observed at the range from 2,319.07–2,358.73 and 3,203.14–3,413.26 shows the N–H and H–O–H molecule, respectively [29]. By TGA spectra, we determine the weight gain or loss due to gas releasing or absorbing as a function of temperature. TGA analysis of used material is indicated by Fig. 5,

which gets two times weight reduction by increasing the temperature from 0 to 800 °C. The first and second weight loss took place by 0.891 mg (13.996%) at the temperature of 127.41 °C and 0.137 mg (2.152%) at 504.79 °C, respectively. It means that the weight loss must be there at more than one point by increasing the temperature. Therefore, it is clear that the material has high hydrophilic nature which can easily absorb moisture from the surrounding atmosphere.

Dielectric properties and impedance measurements were made from 75 kHz to 5 MHz. The sample was pressed into the circular pallet and coated with silver paste on the adjacent faces which, thereby, forms parallel plate capacitor geometry and then the values of  $Z$ ,  $\theta$ , and  $C_p$  has been easily recorded. With the help of these recorded data, various dielectric parameters are calculated and it shows in Fig. 6. Dielectric loss has been calculated by the formula:

$$\tan \delta = 1/\tan \theta$$

where  $\tan \delta$  is dielectric loss tangent which is proportional to the loss of energy of applied field into the sample (this energy is dissipated as heat), and therefore, it is denoted as dielectric loss. The ac conductivity of sample was determined by the relation:  $\sigma_{ac} = \epsilon \omega \tan \delta$ , where  $\omega$  is the angular frequency. Real part and imaginary part of impedance were also calculated by using the given formulas:

$$Z' = Z \cos \theta \text{ and } Z'' = Z \sin \theta \quad (6)$$

Therefore, from the graph, we can easily calculate dielectric constant with respect to the frequency and we obtained a frequency dependent behavior which

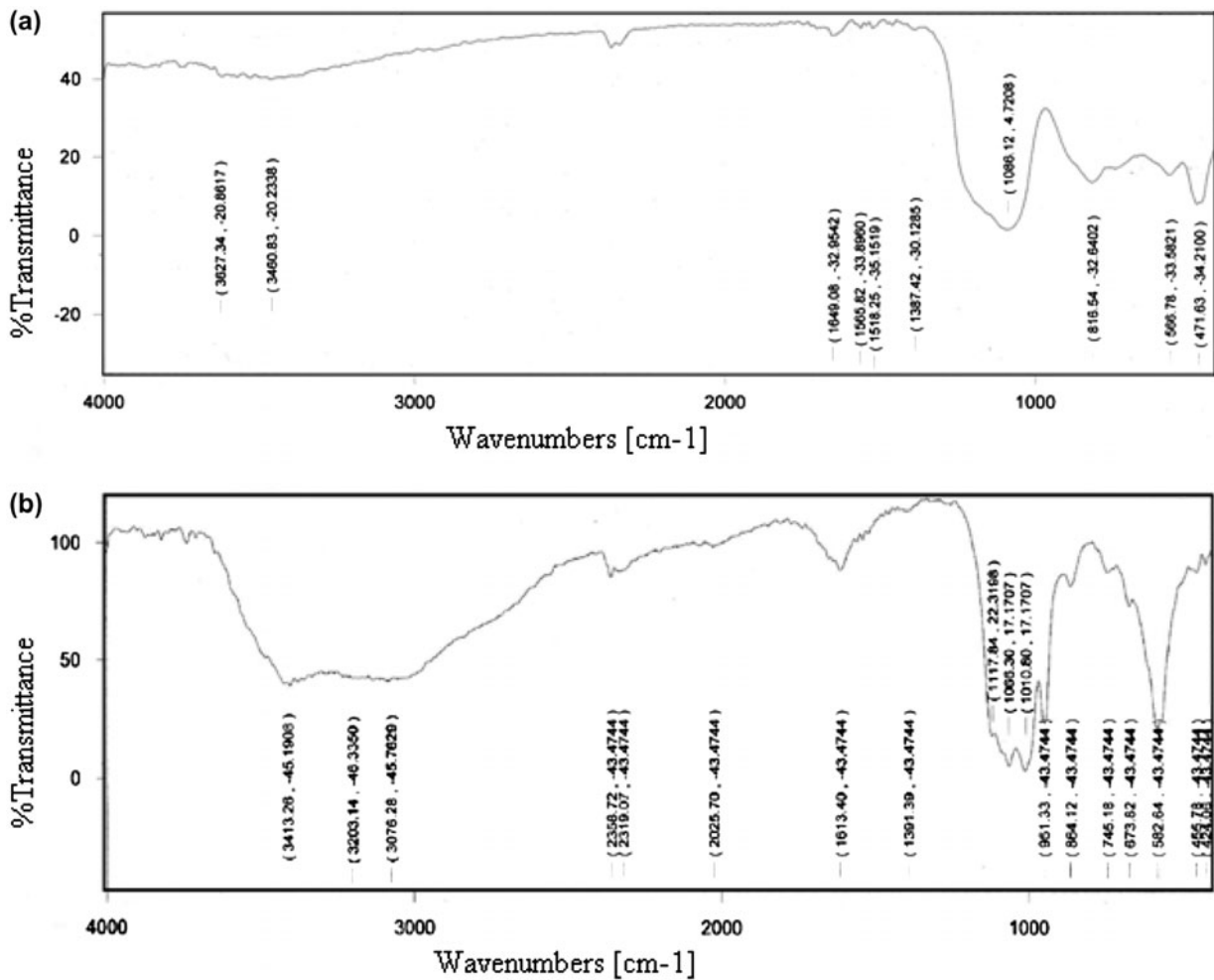


Fig. 4. (a) FTIR spectra of pure PVC, 1 and (b) FTIR spectra of PVC based MP composite material.

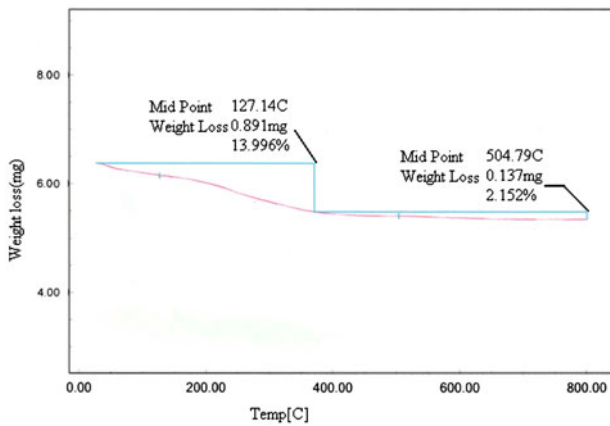


Fig. 5. TGA curve of PVC based MP composite membrane.

indicated that the dielectric constant decreases with increasing frequency. While dielectric loss shows the

complementary result with respect to dielectric constant, it is also indicated by the graph that the dielectric loss is proportional to dielectric constant. By the graph, it is also clear that the real part of impedance shows frequency dependent behavior at low frequency but at the frequency near about 50 MHz and above it shows frequency independent behavior. The imaginary part of impedance also shows the similar result from the real part of impedance, but it shows frequency independent behavior at higher frequency than the real part of impedance.

The thickness swelling, porosity, and water content capability of composite membrane are clearly summarized in Table 1. The water content property of a membrane is totally associated with pressure of water vapor from the surrounding atmosphere. The information about pore size distribution and water structure might be contributed to categorize the particular type of membrane which shows a solution-diffusion, a

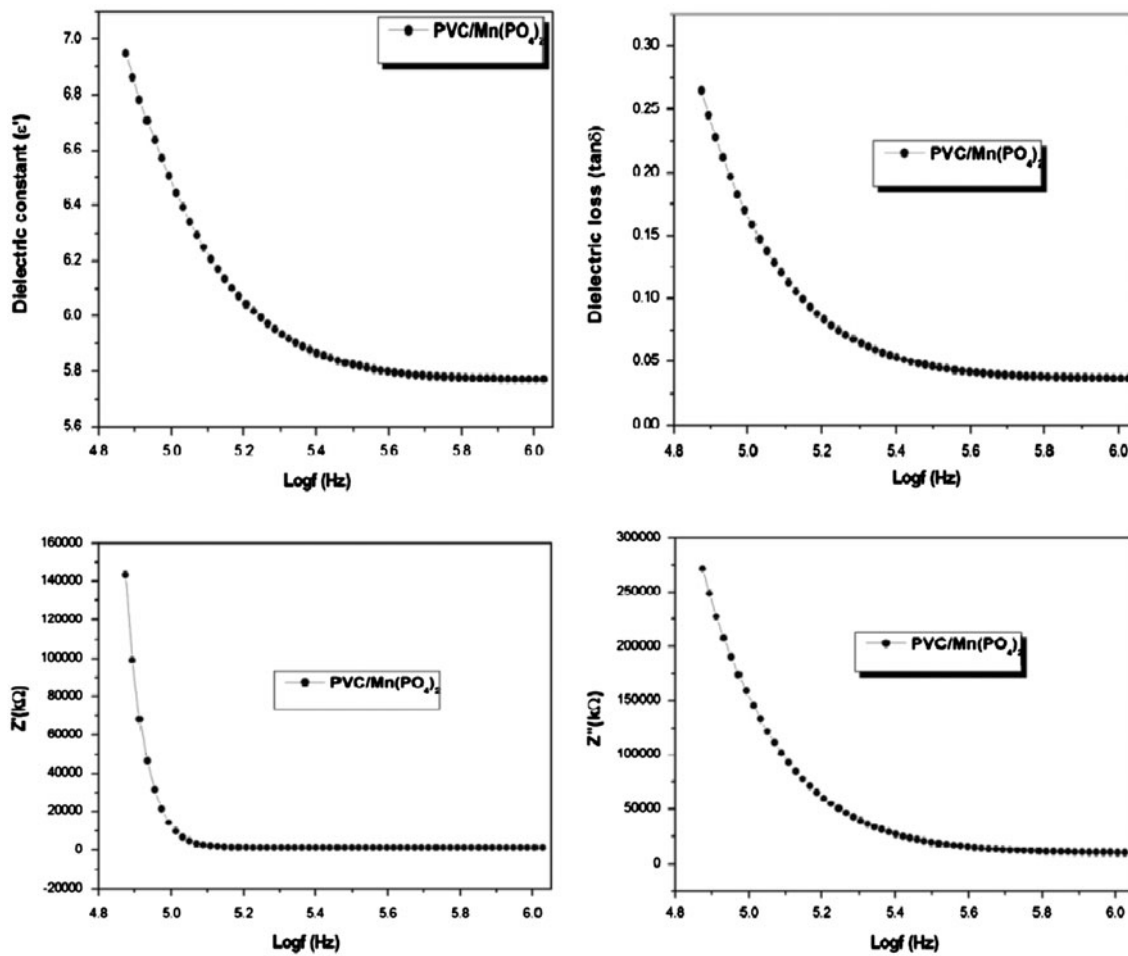


Fig. 6. Dielectric behavior of PVC based MP composite membrane.

Table 1

Thickness, water content, porosity and swelling properties of PVC based MP composite membrane

Applied pressure (MPa)	Thickness of membrane (cm)	Water content as % weight of wet membrane	Porosity	Swelling of % wet membrane
100	0.80	0.056	0.065	No swelling

fine-porous or coarse-porous type membrane [30,31]. The low order of water content, swelling, and porosity with less thickness of membrane suggested that the interstices are insignificant and diffusion within the membrane would happen mostly through the exchange sites. The PVC based MP membrane has been tested for chemical resistance through incubating into acidic, basic, and strongly oxidant media. In acidic as well as alkaline medium, a few considerable modifications have been observed after passing 12, 24, 36, and 48 h consecutively which represents that the membrane can be effective in the above media. In

strong oxidant media, the membrane has become weak in 36 h and can break after 48 h, which shows that it has lost its mechanical resistance after passing more than the given time.

The observed potential data of membrane in contact with various uni-univalent electrolyte solutions is given in Table 2. The values of ionic potential decreases with an increase of solution concentrations, which makes it clear that the membrane follows positive potential order. So, it is indicated that the membrane has cation selective i.e. negatively charged nature. The selectivity is directly proportional with

Table 2

Observed membrane potential for PVC based MP composite membrane in contact with various 1:1 electrolyte solutions

Applied pressure 100 (MPa)			
Observed potential (mV)			
Conc. (mol/L)	KCl	NaCl	LiCl
1	4.2	12.5	16.6
0.1	8.2	26.5	28.5
0.01	12.2	33.0	34.6
0.001	21.4	40.0	42.3
0.0001	32.5	46.0	48.4

dilution through the structural changes which is created by the electrical double layer of solution and membrane boundary [32]. The obtained potential data is plotted as a function of  $-\log C_2$  and it is represented by Fig. 7. The variation in selectivity nature of membrane is due to the adsorption of particular ions which leads to a condition in which the membrane surface behaves as a cation selective nature due to the presence of net negative charge. So, the inorganic precipitated composite membrane has the capability to create potential due to interphases among electrolyte solutions of having unequal concentrations [33].

The charge of the membrane plays a vital role in the adsorption and transportation of simple electrolytes. In synthetic as well as ordinary membranes, there are some significant electrochemical properties to be found, the most important one being the

differences in permeability of co-ions, counter ions, and neutral molecules. The number of charge needed to generate the potential in dilute solution is small and it totally depends on the porosity of membrane [34]. If the pores of membrane are broad many sum of charges are generated good potential whereas on the other hand if they are narrow then a little quantity of charges can give rise to appropriate potential values. Therefore, it is clear that the transport mechanism of simple electrolytes within the charged membrane appear to be incomplete without the evaluation of thermodynamically-effective fixed charge density [35,36]. The membrane which carries various charge densities must follow the order of  $\bar{D} \leq 1$ . Fig. 8. shows the theoretical and observed potential values through solid and broken line, respectively, and it is plotted as a function of  $-\log C_2$ . The coinciding position appearing in figure of various used electrolytes system gives the value of charge density  $\bar{D}$  which is represented in Table 3.

The surface charge density of membrane is found to depend on the initial stage of material preparation. So the order of charge densities were found to be  $KCl > NaCl > LiCl$ , respectively. It is higher in case of KCl than the NaCl due to the size factor of used salts i.e. the smaller size shows the larger ionic atmosphere. The TMS Eq. (1) can also be expressed by the sum of  $\Delta\psi_{Don}$  and  $\Delta\psi_{Diff}$  within the membrane [37,38].

$$\Delta\bar{\psi}_{m,e} = \Delta\psi_{Don} + \Delta\bar{\psi}_{diff} \tag{7}$$

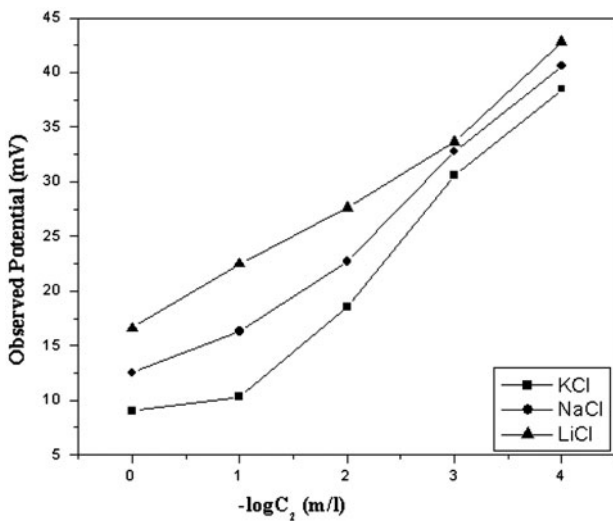


Fig. 7. Plots of observed membrane potentials against logarithm of concentration for PVC based MP composite membrane.

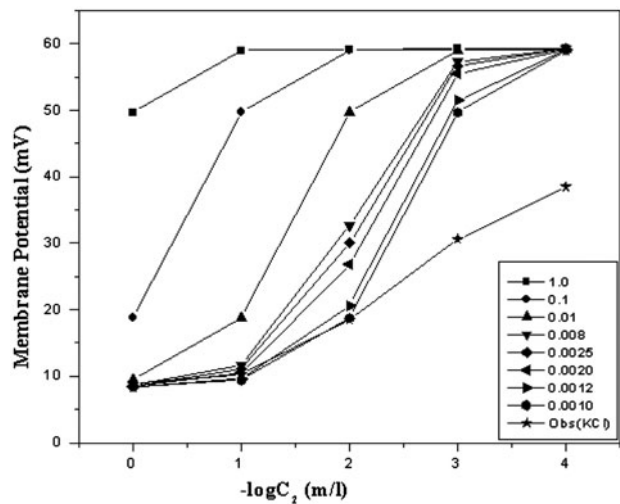


Fig. 8. Plots of membrane potential (theoretical and observed) against logarithm of concentration of KCl electrolyte solution for PVC based MP composite membrane.



Table 3  
Derived values of membrane charge density ( $\bar{D} \times 10^{-3}$  eq/L) of PVC based MP composite membrane

Applied pressure (MPa)	KCl	NaCl	LiCl
100	9.617	9.878	9.66

$$\Delta\psi_{\text{Don}} = -\frac{RT}{V_k F} \ln \left( \frac{\gamma_{2\pm} C_2 \bar{C}_{1+}}{\gamma_{1\pm} C_1 \bar{C}_{2+}} \right) \quad (8)$$

$R$ ,  $T$ , and  $F$  have their usual meanings,  $\gamma_{1\pm}$  and  $\gamma_{2\pm}$  are mean ionic activity coefficients,  $\bar{C}_{1\pm}$  and  $\bar{C}_{2\pm}$  are cation concentration in membrane phase first and second, respectively. The cation concentration is given by the following equation:

$$\bar{C}_+ = \sqrt{\left( \frac{V_x \bar{D}}{2V_k} \right)^2 \left( \frac{\gamma_{\pm} C}{q} \right)^2 - \frac{V_x \bar{D}}{2V_k}} \quad (9)$$

where  $V_k$  and  $V_x$  is the valency of cation and fixed-charge group on membrane matrix, and  $q$  is the charge effectiveness of membrane and it is defined by the equation:

$$q = \sqrt{\frac{\gamma_{\pm}}{K_{\pm}}} \quad (10)$$

$K_{\pm}$  is the distribution coefficient which is expressed as:

$$K_{\pm} = \frac{\bar{C}_i}{C_i}, \bar{C}_i = C_i - \bar{D} \quad (11)$$

$\bar{C}_i$  and  $C_i$  is  $i$ th ion concentration in membrane phase and external solution, respectively. The transport property of electrolytes in membrane phase has been controlled by ion distribution coefficients which appear in Eq. (11). The distribution coefficient was found to be low at lower concentration, and as the concentration of solutions increases, the value significantly increases, and thereafter a stable trend has been followed.

The diffusion potential is expressed as follows:

$$\Delta\bar{\psi}_{\text{diff}} = -\frac{RT\bar{\omega} - 1}{V_k F \bar{\omega} + 1} \times \ln \left( \frac{(\bar{\omega} + 1)\bar{C}_2 + (V_x/V_k)\bar{D}}{(\bar{\omega} + 1)\bar{C}_1 + (V_x/V_k)\bar{D}} \right) \quad (12)$$

where  $\bar{\omega} = \bar{u}/\bar{v}$  is mobility ratio of cation towards anion in membrane phase. Therefore, the total

membrane potential has been obtained by the following equation:

$$\Delta\bar{\psi}_{m,e} = -\frac{RT}{V_k F} \ln \left( \frac{\gamma_{2\pm} C_2 \bar{C}_{1+}}{\gamma_{1\pm} C_1 \bar{C}_{2+}} \right) - \frac{RT\bar{\omega} - 1}{V_k F \bar{\omega} + 1} \times \ln \left( \frac{(\bar{\omega} + 1)\bar{C}_2 + (V_x/V_k)\bar{D}}{(\bar{\omega} + 1)\bar{C}_1 + (V_x/V_k)\bar{D}} \right) \quad (13)$$

To the applicability of theoretical equation for system, the donnan and diffusion potentials are separately calculated with the help of observed potential measurements [39,40]. The transport property of ions is an important parameter to investigate the further study of membrane, which is represented by the equation:

$$\Delta\bar{\psi}_m = -\frac{RT}{F} (t_+ - t_-) \ln \frac{C_2}{C_1} \quad (14)$$

where

$$\frac{t_+}{t_-} = \frac{\bar{u}}{\bar{v}} \quad (15)$$

To get the values of transport number, Eq. (14) is used, and subsequently the mobility ratio  $\bar{\omega} = \bar{u}/\bar{v}$  can also be calculated by the observed potential data. The mobility ratio was found to follow KCl < NaCl < LiCl order and it is clearly shown by Fig. 9. The high mobility ratio is due to the higher transport number of comparatively free cations of electrolytes, whereas similar trend of mobility ratio is also seen in least

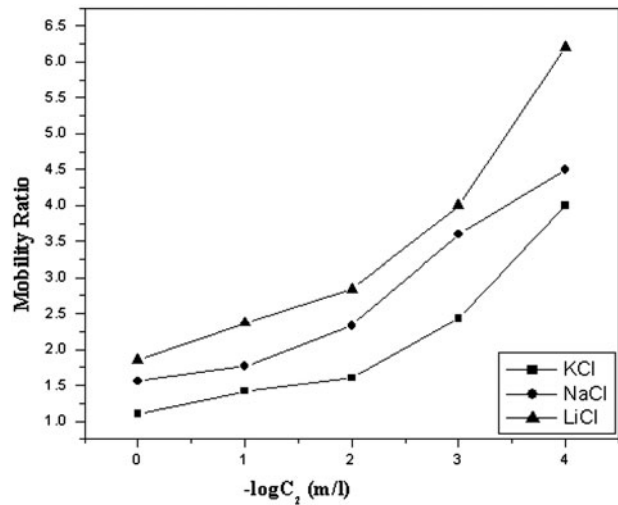


Fig. 9. Plot for mobility ratio of PVC based MP composite membrane for 1:1 electrolytes against concentration.

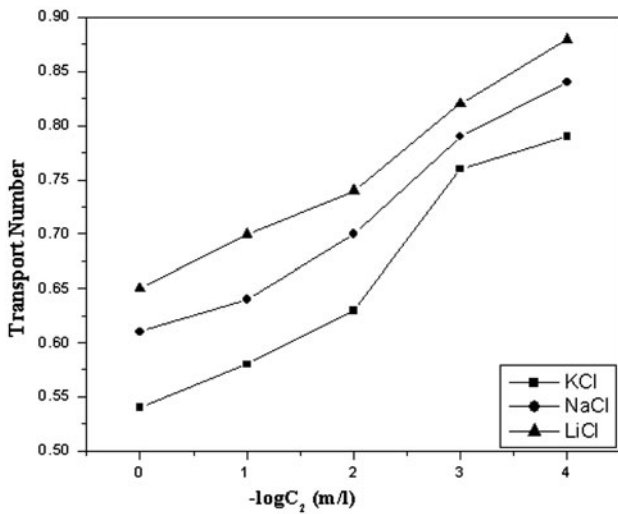


Fig. 10. Plots showing the transport number of cation for the PVC based MP composite membrane for 1:1 electrolytes against concentration.

concentrated solutions. The transport number of used electrolytes also follows the increasing order like KCl < NaCl < LiCl which is clearly shown by Fig. 10. Donnan and diffusion potential has been calculated by

Table 4

The values of  $t_+$ ,  $\bar{U}$ ,  $\bar{\omega}$  and  $K_{\pm}, q, \bar{C}_+$  for various electrolytes at different concentrations of PVC based MP composite membrane

$C_2$ (mol/L)	$t_+$	$\bar{U}$	$\bar{\omega}$	$K_{\pm}$	$q$	$\bar{C}_+$
<i>KCl (electrolyte)</i>						
1.000	0.54	0.08	1.17	0.9910	1.010	0.99105
0.1000	0.57	0.14	1.32	0.9010	1.110	0.09121
0.0100	0.61	0.22	1.56	0.4050	2.500	0.00345
0.0010	0.69	0.38	2.22	-8.600	0.100	0.00045
0.0001	0.78	0.56	3.54	-95.00	0.010	0.00005
<i>NaCl</i>						
1.000	0.61	0.22	1.56	0.9906	1.010	0.99135
0.1000	0.73	0.46	2.70	0.9050	1.104	0.09146
0.0100	0.78	0.56	3.54	0.5300	1.886	0.00290
0.0010	0.84	0.68	5.20	-8.400	0.119	0.00030
0.0001	0.89	0.78	8.09	-93.00	0.010	0.00002
<i>LiCl</i>						
1.000	0.65	0.30	1.85	0.9900	1.010	0.99165
0.1000	0.75	0.50	3.00	0.9000	1.111	0.91832
0.0100	0.80	0.60	4.00	0.0940	10.638	0.00327
0.0010	0.86	0.72	6.14	-8.000	0.125	0.00030
0.0001	0.90	0.80	9.00	-89.60	0.011	0.00004

using the parameters  $\gamma_{1\pm}, \gamma_{2\pm}, \bar{C}_{1+}, \bar{C}_{2+}, \bar{\omega}, V_x, V_k$ . The experimentally derived values of charge density are also calculated with the help of Eqs. (8) and (12). The values of parameters like  $K_{\pm}, q,$  and  $\bar{C}_+$  are also derived for the system and it is represented by Table 4.

### 6. Conclusion

The PVC based MP composite membrane was effectively prepared by sol-gel method of material preparation and it is found to be of a quite stable nature. The fixed-charge density is the central parameter that governs the transport phenomena of composite membrane and it depends on the feed composition and applied pressure. The structural characterization details of membrane shows great properties in terms of thickness, porosity, mobility ratio, and effective charge density. The membrane potential of PVC based MP composite membrane for different 1:1 electrolytes was found to follow an increasing order of KCl < NaCl < LiCl while the surface charge density follows the reverse order of observed potential values.

### Acknowledgment

The authors gratefully acknowledge the Chairman, Department of Chemistry, Aligarh Muslim University, Aligarh-India for providing necessary research facilities. We are also thankful to the UGC for financial assistance, USIF-AMU, Aligarh for scanning electron microscopy and Department of Applied Physics for XRD analysis.

### Nomenclature

- AR — analytical reagent
- $C_1, C_2$  — concentrations of electrolyte solution on either side of the membrane (mol/L)
- $\bar{C}_{1+}$  — cation concentration in membrane phase 1 (mol/L)
- $\bar{C}_{2+}$  — cation concentration in membrane phase 2 (mol/L)
- $C_i$  —  $i$ th ion concentration of external solution (mol/L)
- $\bar{C}_i$  —  $i$ th ion concentration in membrane phase (mol/L)
- $\bar{D}$  — charge density in membrane (eq/L)
- $F$  — Faraday constant (C/mol)
- 100 MPa — pressure (MPa)
- $q$  — charge effectiveness of the membrane
- $R$  — gas constant (J/K/mol)
- SCE — saturated calomel electrode

TMS	—	Teorell, Meyer, and Sievers
$t_+$	—	transport number of cation
$t_-$	—	transport number of anion
$\bar{u}$	—	mobility of cations in the membrane phase ( $\text{m}^2/\text{v/s}$ )
$\bar{v}$	—	mobility of anions in the membrane phase ( $\text{m}^2/\text{v/s}$ )
$V_k$	—	valency of cation
$V_x$	—	valency of fixed-charge group
$\bar{U}$	—	$\bar{U} = (\bar{u} - \bar{v})/(\bar{u} + \bar{v})$
MP	—	manganous Phosphate
SEM	—	scanning electron microscopy
FTIR	—	Fourier transform infrared spectroscopy
XRD	—	X-ray diffraction
TGA	—	thermogravimetric analysis
DTA	—	differential thermal analysis
LCR	—	inductance, capacitance, and resistance

#### Greek symbols

$\gamma_{\pm}$	—	mean ionic activity coefficients
$\bar{\omega}$	—	mobility ratio
$\Delta\psi_m$	—	observed membrane potential (mV)
$\Delta\bar{\psi}_m$	—	theoretical membrane potential (mV)
$\Delta\psi_{\text{Don}}$	—	Donnan potential (mV)
$\Delta\psi_{\text{diff}}$	—	diffusion potential (mV)

#### References

- M.N. Beg, M.A.Z. Matin, Studies with nickel phosphate membranes: Evaluation of charge density and test of recently developed theory of membrane potential, *J. Membr. Sci.* 196 (2002) 95–102.
- J. Balster, O. Krupenko, I. Punt, D.F. Stamatialis, M. Wessling, Preparation and characterisation of monovalent ion selective cation exchange membranes based on sulphonated poly (ether ether ketone), *J. Membr. Sci.* 263 (2005) 137–145.
- R. Scherer, A.M. Bernardes, M.M.C. Forte, J.Z. Ferreira, C.A. Ferreira, Preparation and physical characterization of a sulfonated poly (styrene-co-divinylbenzene) and polypyrrole composite membrane, *Mater. Chem. Phys.* 71 (2001) 131–136.
- M.M.A. Khan, Rafiuddin, Inamuddin, Electrochemical characterization and transport properties of polyvinyl chloride based carboxy methyl cellulose Ce(IV) molybdophosphate composite cation exchange membrane, *J. Ind. Eng. Chem.* 18 (2012) 1391–1397.
- M. Arsalan, Rafiuddin, Fabrication, characterization, transportation of ions and antibacterial potential of polystyrene based  $\text{Cu}_3(\text{PO}_4)_2/\text{Ni}_3(\text{PO}_4)_2$  composite membrane, *J. Ind. Eng. Chem.* 20 (2014) 3568–3577.
- T. Arfin, Rafiuddin, An electrochemical and theoretical comparison of ionic transport through a polystyrene-based cobalt arsenate membrane, *Electrochim. Acta* 56 (2011) 7476–7483.
- R. Schöllhorn, Intercalation systems as nanostructured functional materials, *Chem. Mater.* 8 (1996) 1747–1757.
- F. Jabeen, Rafiuddin, Transport studies with composite membrane by sol-gel method, *J. Dispersion Sci. Technol.* 31 (2010) 1708–1713.
- Y. Wang, N. Herron, X-ray photoconductive nanocomposites, *Science* 273 (1996) 632–634.
- S. Higashika, K. Kimura, Y. Matsuo, Y. Sugie, Synthesis of polyaniline-intercalated graphite oxide, *Carbon* 37 (1999) 354–356.
- P. Pandey, R.S. Chauhan, Membranes for gas separation, *Prog. Polym. Sci.* 26 (2001) 853–893.
- M.Y. Kariduraganavar, R.K. Nagarale, A.A. Kittur, S.S. Kulkarni, Ion-exchange membranes: Preparative methods for electro dialysis and fuel cell applications, *Desalination* 197 (2006) 225–246.
- Md. Ramir Khan, Rafiuddin, Synthesis, characterization and properties of polystyrene incorporated calcium tungstate membrane and studies of its physicochemical and transport behavior, *J. Mol. Struct.* 1033 (2013) 145–153.
- M. Amara, H. Kerdjoudj, Water reuse of an industrial effluent by means of electro deionisation, *Desalination* 167 (2003) 49–54.
- C. Hegde, A.M. Isloor, M. Padaki, P. Wanichapichart, Y. Liangdeng, Synthesis and performance characterization of PS-PPEES nanoporous membranes with nonwoven porous support, *Arab. J. Chem.* 6 (2013) 319–326.
- A. Cañas, M.J. Ariza, J. Benavente, Characterization of active and porous sub layers of a composite reverse osmosis membrane by impedance spectroscopy, streaming and membrane potentials, salt diffusion and X-ray photoelectron spectroscopy measurements, *J. Membr. Sci.* 183 (2001) 135–146.
- B. van der Bruggen, J. Schaep, D. Wilms, C. Vandecasteele, Influence of molecular size, polarity and charge on the retention of organic molecules by nanofiltration, *J. Membr. Sci.* 156 (1999) 29–41.
- W. Pusch, A. Tanioka, Structure investigations of homogeneous cellulose acetate membranes by gas permeation measurements, *Desalination* 46 (1983) 425–434.
- V.K. Shahi, G.S. Trivedi, S.K. Thamby, R. Rangarajan, Studies on the electrochemical and permeation characteristics of asymmetric charged porous membranes, *J. Colloid Interface Sci.* 262 (2003) 566–573.
- M.M.A. Khan, Rafiuddin, Synthesis, characterization and electrochemical study of calcium phosphate ion-exchange membrane, *Desalination* 272 (2011) 306–312.
- U. Ishrat, Rafiuddin, Synthesis characterization and electrical properties of titanium molybdate composite membrane, *Desalination* 286 (2012) 8–15.
- F.A. Siddiqi, M.N. Beg, S.P. Singh, Studies with model membranes. X. Evaluation of the thermodynamically effective fixed charge density and permselectivity of mercuric and cupric iodide parchment-supported membranes, *J. Polym. Sci.* 15 (1979) 959–972.
- H. Matsumoto, A. Tanioka, T. Murata, M. Higa, K. Horiuchi, Effect of proton on potassium ion in countertransport across fine porous charged membranes, *J. Phys. Chem. B* 102 (1998) 5011–5016.
- L.J. Ghanshyam, P.S. Singh, Synthesis of novel silica-polyamide nanocomposite membrane with enhanced properties, *J. Membr. Sci.* 328 (2009) 257–267.
- M. Arsalan, M.M.A. Khan, Rafiuddin, A comparative study of theoretical, electrochemical and ionic transport through PVC based  $\text{Cu}_3(\text{PO}_4)_2$  and polystyrene supported  $\text{Ni}_3(\text{PO}_4)_2$  composite ion exchange porous membranes, *Desalination* 318 (2013) 97–106.

- [26] S. Weqar, A. Khan, A. Shakeel, Inamuddin, Synthesis, characterization and ion-exchange properties of a new and novel 'organic-inorganic' hybrid cation-exchanger: Poly(methyl methacrylate) Zr (IV) phosphate, *Colloids Surf.* 295 (2007) 193–199.
- [27] M. Arsalan, Rafiuddin, Fabrication, characterization, transportation of ions and antibacterial potential of polystyrene based  $\text{Cu}_3(\text{PO}_4)_2/\text{Ni}_3(\text{PO}_4)_2$  composite membrane, *J. Ind. Eng. Chem.* 20 (2014) 3568–3577.
- [28] F.J. Rafiuddin, Membrane potential and fixed charge density across  $\text{TiPO}_4\text{-VPO}_4$  composite membranes for uni-univalent electrolyte solution, *J. Por. Mat.* 16 (2009) 257–265.
- [29] M. Arsalan, Rafiuddin, Synthesis, structural characterization, electrochemical, and electrical study of polystyrene based manganous tungstate composite cation exchange membrane, *Desalin. Water Treat.* doi: 10.1080/19443994.2013.831793.
- [30] T. Arfin, Rafiuddin, Transport studies of nickel arsenate membrane, *J. Electroanal. Chem.* 636 (2009) 113–122.
- [31] M. Arsalan, Rafiuddin, Binding nature of polystyrene and PVC 50:50% with CP and NP 50:50% ion exchangeable, mechanically and thermally stable membrane, *J. Ind. Eng. Chem.* 20 (2014) 3283–3291.
- [32] A.A. Khan, Inamuddin, Preparation and characterization of a new organic-inorganic nano-composite poly-o-toluidine Th(IV) phosphate: Its analytical applications as cation-exchanger and in making ion-selective electrode, *Talanta* 72 (2007) 699–710.
- [33] B.P. Tripathi, V.K. Shahi, Organic-inorganic nanocomposite polymer electrolyte membranes for fuel cell applications, *Prog. Polym. Sci.* 36 (2011) 945–979.
- [34] R.K. Nagarale, V.K. Shahi, S.K. Thampy, R. Rangarajan, Studies on electrochemical characterization of polycarbonate and polysulfone based heterogeneous cation-exchange membranes, *React. Funct. Polym.* 61 (2004) 131–138.
- [35] H. Zou, S. Wu, J. Shen, Polymer/silica nanocomposites: Preparation, characterization, properties, and applications, *Chem. Rev.* 108 (2008) 3893–3957.
- [36] M.M. Hassan, A.S. Ahmed, M. Chaman, W. Khan, A.H. Naqvi, A. Azam, Structural and frequency dependent dielectric properties of  $\text{Fe}^{3+}$  doped ZnO nanoparticles, *Mater. Res. Bull.* 47 (2012) 3952–3958.
- [37] T. Arfin, Rafiuddin, Electrochemical properties of titanium arsenate membrane, *Electrochim. Acta* 54 (2009) 6928–6934.
- [38] H. Matsumoto, A. Tanioka, T. Murata, M. Higa, K. Horiuchi, Effect of proton on potassium ion in countertransport across fine porous charged membranes, *J. Phys. Chem. B* 102 (1998) 5011–5016.
- [39] T.J. Chou, A. Tanioka, Membrane potential of composite bipolar membrane in ethanol-water solutions: The role of membrane interface, *J. Colloid Interface Sci.* 212 (1999) 293–300.
- [40] S.A. Nabi, M. Naushad, Synthesis and characterization of a new inorganic cation exchanger Zr(IV) tungstomolybdate: Analytical applications for metal content determination in real sample and synthetic mixture, *J. Hazard. Mater.* 142 (2007) 404–411.